

# Deglycosylation, processing and crystallization of human testis angiotensin-converting enzyme

Kerry GORDON\*, Pierre REDELINGHUYTS\*, Sylva L. U. SCHWAGER\*, Mario R. W. EHLERS\*<sup>1</sup>, Anastassios C. PAPAGEORGIU†<sup>2</sup>, Ramanathan NATESH†, K. Ravi ACHARYA† and Edward D. STURROCK\*<sup>†,3</sup>

\*Division of Medical Biochemistry, Faculty of Health Sciences, University of Cape Town, Observatory 7925, South Africa, †Department of Biology and Biochemistry, University of Bath, Claverton Down, Bath BA2 7AY, U.K., and ‡MRC/UCT Liver Research Centre, Faculty of Health Sciences, University of Cape Town, Observatory 7925, South Africa

Angiotensin I-converting enzyme (ACE) is a highly glycosylated type I integral membrane protein. A series of underglycosylated testicular ACE (tACE) glycoforms, lacking between one and five N-linked glycosylation sites, were used to assess the role of glycosylation in tACE processing, crystallization and enzyme activity. Whereas underglycosylated glycoforms showed differences in expression and processing, their kinetic parameters were similar to that of native tACE. N-glycosylation of Asn-72 or Asn-109 was necessary and sufficient for the production of enzymically active tACE but glycosylation of Asn-90 alone resulted in rapid intracellular degradation. All mutants showed similar levels of phorbol ester stimulation and were solubilized at the same juxtamembrane cleavage site as the native enzyme. Two mutants, tACE $\Delta$ 36-g1234 and -g13, were successfully crystal-

lized, diffracting to 2.8 and 3.0 Å resolution respectively. Furthermore, a truncated, soluble tACE (tACE $\Delta$ 36NJ), expressed in the presence of the glucosidase-I inhibitor *N*-butyldeoxynojirimycin, retained the activity of the native enzyme and yielded crystals belonging to the orthorhombic P2<sub>1</sub>2<sub>1</sub>2<sub>1</sub> space group (cell dimensions, a = 56.47 Å, b = 84.90 Å, c = 133.99 Å,  $\alpha = 90^\circ$ ,  $\beta = 90^\circ$  and  $\gamma = 90^\circ$ ). These crystals diffracted to 2.0 Å resolution. Thus underglycosylated human tACE mutants, lacking O-linked oligosaccharides and most N-linked oligosaccharides or with only simple N-linked oligosaccharides attached throughout the molecule, are suitable for X-ray diffraction studies.

**Key words:** angiotensin I-converting enzyme (ACE), crystallization, ectodomain shedding, glycosylation.

## INTRODUCTION

Angiotensin I-converting enzyme (ACE; EC 3.4.15.1) is a key regulatory enzyme in cardiovascular pathophysiology. It is a pivotal component of the renin-angiotensin system, converting the inactive decapeptide angiotensin I to the octapeptide angiotensin II, a potent vasoconstrictor and a trigger for aldosterone release. In addition, ACE inactivates the vasodilator bradykinin and hence it is essential for regulating blood pressure and fluid homeostasis. There are two distinct forms of ACE: somatic ACE, which is present in brush-border epithelial cells and endothelial cells; and the smaller germinal form, which is present only in spermatozoa and is important in fertility. More recently, an ACE homologue, ACE2, has emerged as another player in the renin-angiotensin system. ACE2 appears to be involved in cardiac function but does not directly affect blood pressure [1,2].

The clinical success of the first-generation ACE inhibitors, such as captopril and enalapril, in the treatment of hypertension and congestive heart failure is well established. However, adverse events, notably persistent cough and skin reactions including angioedema, occur in up to 20% of subjects, limiting more widespread use. Although angiotensin receptor blockers present an alternative, their therapeutic profile is not identical to that of the ACE inhibitors. First-generation ACE inhibitors were de-

veloped before it was realized that somatic ACE consists of two homologous domains, the N and C domains, each containing an active site. Biochemical and genetic studies have indicated that the active sites are distinct and non-redundant. Therefore, highly domain-selective ACE inhibitors may offer novel therapeutic profiles.

The search for more selective inhibitors has proven difficult due to the lack of a three-dimensional structure of the enzyme. Limited success has been achieved using three-dimensional quantitative structure–activity relationship studies [3] and NMR [4] studies. However, the rational design of domain-selective inhibitors requires more detailed information about the active site and the interaction of inhibitors with the various subsites, necessitating a high-resolution structure of the protein. Crystallization of ACE suitable for X-ray diffraction will likely require removal or modification of the protein's carbohydrates.

Previously, we have shown that inhibition of complex oligosaccharide formation by the glucosidase-I inhibitor *N*-butyldeoxynojirimycin (NB-DNJ) led to the production of an active glycoform [tACE $\Delta$ 36NJ]; testicular ACE (tACE) lacking N-terminal 36 residues (tACE $\Delta$ 36) and C-terminal cytoplasmic and transmembrane domains] that was electrophoretically homogeneous and a good candidate for crystallographic studies [5].

Abbreviations used: ACE, angiotensin I-converting enzyme; tACE, testicular ACE; tACE-wt, wild-type tACE; tACE $\Delta$ 36, tACE lacking N-terminal 36 residues; tACE $\Delta$ 36NJ, tACE $\Delta$ 36 lacking C-terminal cytoplasmic and transmembrane domains; CHO, Chinese hamster ovary; Hip-His-Leu, hippuryl-L-histidyl-L-leucine; MALDI-TOF, matrix-assisted laser-desorption ionization–time-of-flight; NB-DNJ, *N*-butyldeoxynojirimycin.

<sup>1</sup> Present address: Pacific Biometrics, Inc., 220 W. Harrison Street, Seattle, WA 98119, U.S.A.

<sup>2</sup> Present address: Turku Centre for Biotechnology, University of Turku and Åbo Akademi University, BioCity, Turku 20521, Finland.

<sup>3</sup> To whom correspondence should be addressed, at the Division of Medical Biochemistry (e-mail sturrock@curie.uct.ac.za).

In this study, we used a combination of site-directed mutagenesis and enzyme kinetics to evaluate further the contribution of the N-glycosylation sites of human tACE to processing and enzymic activity, and to investigate whether these mutant proteins are suitable for crystallization and X-ray diffraction studies. Here we report for the first time the crystallization of tACE $\Delta$ 36NJ and of the tACE glycosylation mutants tACE $\Delta$ 36-g1234 and -g13.

## MATERIALS AND METHODS

### Construction of glycosylation mutants

Minimally glycosylated isoforms of human tACE were constructed by disrupting combinations of six of the seven potential N-linked glycosylation sites. Glycosylation was disrupted by site-directed mutagenesis of the site of attachment in the recognition sequon (Asn-Xaa-Ser/Thr) through a conserved substitution of the Asn to a Gln residue. A truncated form of tACE, lacking the first 36 N-terminal residues (tACE $\Delta$ 36), was used for the construction of all mutants [5]. tACE $\Delta$ 36 cDNA was divided into four fragments and introduced into pGEM-11Zf(+) (Gene-Editor; Promega) to facilitate site-directed mutagenesis. An *Eco*47III site was introduced into pGEM-11Zf(+) for cloning of the first and second tACE $\Delta$ 36 fragments. A 146 bp *Bam*HI/*Nhe*I-

digested pBR329 fragment that contained an *Eco*47III site was ligated to *Bam*HI/*Xba*I-digested pGEM. The following forward (F) and reverse (R) mutagenic oligonucleotides were used for altering the consensus sites for N-linked glycosylation: g1-F, g2-F, g3-F, g4-F, g5-F, g6-F, g1-R, g2-R and g3-R, with the number referring to each complementary recognition sequon: 1 (Asn-72), 2 (Asn-90), 3 (Asn-109), 4 (Asn-155), 5 (Asn-337) and 6 (Asn-586; Figure 1). In the first fragment, a cDNA containing a mutation at one site served as a template for the mutagenesis of the second site, thus generating five variants with either one or two sites out of the first three eliminated. The fourth, fifth and sixth sites (Asn-155, Asn-337 and Asn-586) were eliminated from fragments 2, 3 and 4, respectively, using primers g4-F, g5-F and g6-F.

The nucleotide sequence of each fragment was confirmed by sequencing to ensure that only the desired mutation had been created. The four fragments were reassembled to produce eight tACE $\Delta$ 36 glycosylation mutants (Figure 1).

The mutants were introduced into the mammalian expression vector pLEN to facilitate the production of underglycosylated tACE $\Delta$ 36 protein. The expression vectors pLEN-tACE $\Delta$ 36g(*n*), where *n* defines the site-numbers that are glycosylated, were stably expressed in Chinese hamster ovary (CHO) cells as described previously [6]. Similarly, wild-type tACE (tACE-wt),

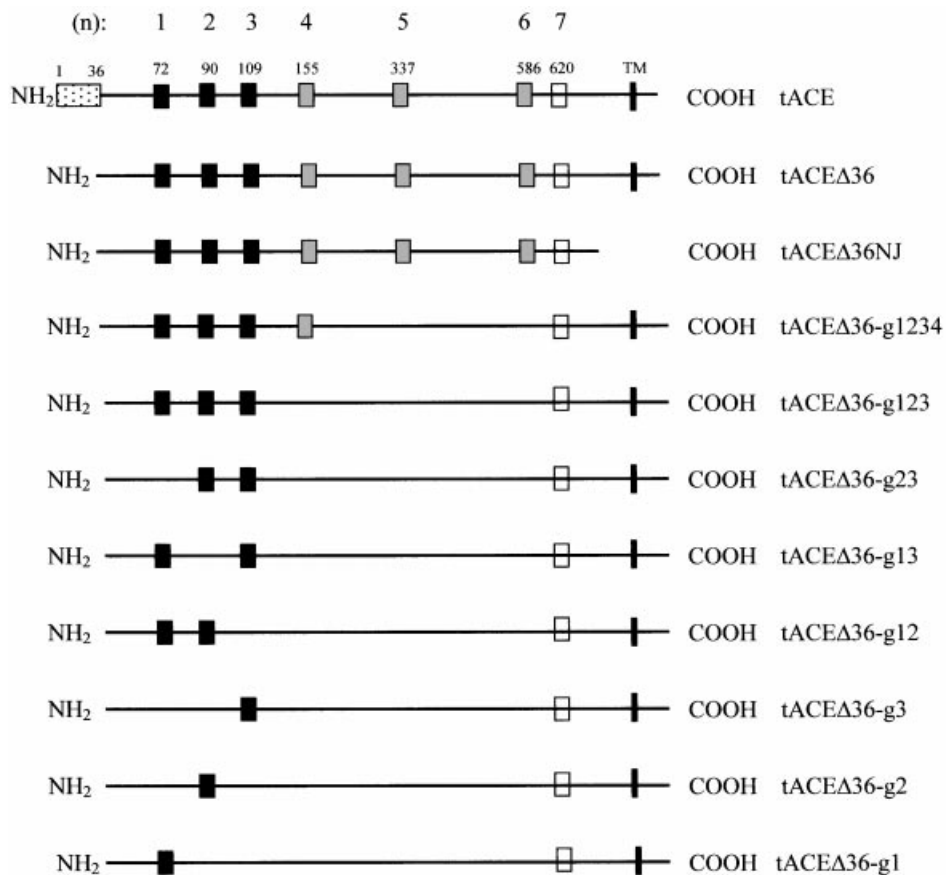


**Figure 1** Schematic representation of tACE $\Delta$ 36 glycosylation mutants

N-glycosylation sites are indicated by boxes: always glycosylated (black), partially glycosylated (grey) and unglycosylated (white), as determined previously [5]; sites (*n*) are numbered 1–7 from the N-terminus. The N-terminal O-glycosylated region is shown as a stippled box. TM, transmembrane domain. Note that although the mutants are expressed with the TM and cytosolic domains (except tACE $\Delta$ 36NJ), these are cleaved from the proteins during cell-mediated shedding.

retaining its 36-residue N-terminus as well as the transmembrane region and juxtamembrane stalk, was stably expressed in CHO cells [7]. A deletion mutant, tACE $\Delta$ 36NJ, truncated after Ser-625, and thus lacking the cytoplasmic and transmembrane domains as well as most of the juxtamembrane stalk, was described previously [5]. The vector pEE14-tACE $\Delta$ 36NJ was transfected into CHO cells, and clones stably expressing the mutant were amplified using methionine sulphoxamine (Sigma), as described in [5].

#### Purification of glycosylation mutants and tACE $\Delta$ 36NJ

The soluble (released) glycosylation mutants were purified from conditioned medium by affinity chromatography on a Sepharose-28-lisinopril affinity resin as described in [6]. CHO cells expressing tACE $\Delta$ 36NJ were grown in GMEM-10 (Life Technologies) containing 10% dialysed fetal bovine serum (Life Technologies) and 1.5 mM NB-DNJ (a gift from Dr F. Platt, University of Oxford, Oxford, U.K.) [5]. Soluble tACE $\Delta$ 36NJ was purified by affinity chromatography on a Sepharose-28-lisinopril affinity resin as described in [6].

#### Western blot analysis of glycosylation mutants

tACE-wt, tACE $\Delta$ 36NJ and tACE $\Delta$ 36-g1, -g2, -g3, -g12, -g13, -g23, -g123 and -g1234 (see Figure 1) were immunodetected by Western blotting of cell lysates and harvested medium from transfected CHO cells. Proteins were separated on SDS/PAGE (10% gels) and transferred to a nitrocellulose membrane (Hybond-C; Amersham Biosciences). The membrane was probed with a polyclonal rabbit anti-human-tACE antibody. The membrane was developed using the ECL chemiluminescence kit (Amersham Biosciences) and visualized on autoradiographic film (Sigma) as per the manufacturer's instructions.

#### Analysis of ectodomain shedding and cleavage sites

After selection for stable transfectants, kinetic analyses of rates of accumulation of soluble (released) ACE activity and changes in membrane-bound ACE activity were performed in the presence and absence of 1  $\mu$ M PMA (Sigma) [8]. Identification of the stalk cleavage sites and analysis of the C-terminal glycosylation site in the released (soluble) protein were carried out using limited proteolysis and matrix-assisted laser-desorption ionization-time-of-flight (MALDI-TOF) MS by methods described previously [8].

#### Determination of kinetic constants for tACE hydrolysis of hippuryl-L-histidyl-L-leucine (Hip-His-Leu)

Enzyme was purified from harvest medium via affinity chromatography on a Sepharose-28-lisinopril affinity resin and rates of substrate hydrolysis were determined. Assays were performed in 100 mM potassium phosphate buffer, pH 8.3, containing 300 mM NaCl. Initial velocities were calculated over a range of Hip-His-Leu (Sigma) concentrations (0.2–5.0 mM) under initial-rate conditions, and fitted to the Michaelis–Menten equation.  $K_m$  and  $V_{max}$  values were determined by non-linear regression analysis. Turnover numbers ( $k_{cat}$ ) and specificity constants ( $k_{cat}/K_m$ ) were determined using a calculated molecular mass of 100 kDa.

#### Crystallization of ACE mutants

The purified tACE $\Delta$ 36NJ and tACE glycosylation mutants were stored at  $-20^\circ\text{C}$  in 10 mM Hepes (Sigma) and 0.1% PMSF

(Sigma). Extensive crystallization trials using commercially available crystal screen conditions (Hampton Research) were attempted. In addition,  $(\text{NH}_4)_2\text{SO}_4$ , poly(ethylene glycol) ('PEG'; Fluka) and 2-methyl-2,4-pentanediol ('MPD'; Sigma) matrices were used. The best crystals for these proteins were grown at  $16^\circ\text{C}$  by the vapour-diffusion hanging-drop method, by mixing 2  $\mu\text{l}$  of the protein solution at  $\approx 11.5$  mg/ml, in 10 mM Hepes and 0.1% PMSF, with an equal volume of a reservoir solution containing 15% poly(ethylene glycol) 4000, 50 mM sodium acetate trihydrate (Sigma), pH 4.7, and 10  $\mu\text{M}$   $\text{ZnSO}_4 \cdot 7\text{H}_2\text{O}$  (Aldrich).

## RESULTS

### Expression of tACE mutants in CHO cells and enzyme kinetics

The role of N-linked glycosylation in the expression and processing of tACE $\Delta$ 36 was investigated to establish the minimum glycosylation requirements for the expression of correctly folded, enzymically active protein. The eight tACE glycosylation mutants were transfected into CHO cells and the effect of deglycosylation on the activity, expression and processing of tACE $\Delta$ 36 was assessed by enzyme assays, immunodetection and cleavage site analysis.

Western blot analysis of cellular and soluble tACE $\Delta$ 36 glycoforms revealed proteins with increased mobility relative to glycosylated tACE-wt (Figure 2), which was dependent on their degree of glycosylation. Furthermore, differences were detected in the expression and processing of the various glycoforms. The levels of tACE $\Delta$ 36-g2 protein were low in the cellular extracts (Figure 2A) and absent from the harvest medium (Figure 2B), suggesting that this mutant was processed defectively and degraded intracellularly. Interestingly, whereas tACE $\Delta$ 36-g1 was expressed in the cells at levels comparable with the other proteins (Figure 2A), processing and solubilization were less efficient than for tACE $\Delta$ 36-g3, -g123 and -g1234 (Figure 2B).

The  $K_m$  and  $k_{cat}$  values obtained for the hydrolysis of Hip-His-Leu by tACE glycoforms (Table 1) were in agreement with those previously published for the C-fragment of the human endothelial isoform ( $K_m = 2.0$  mM) [9]. Differences in the kinetic constants, in particular the specificity constants of glycosylated and underglycosylated tACE $\Delta$ 36 mutants, were not considered sufficiently different to reflect major alterations in the conformation and activity of the protein. Glycosylation of tACE $\Delta$ 36 at one (tACE $\Delta$ 36-g3) or two (tACE $\Delta$ 36-g13) N-terminal glycosylation sequons was sufficient to maintain the functional integrity of the

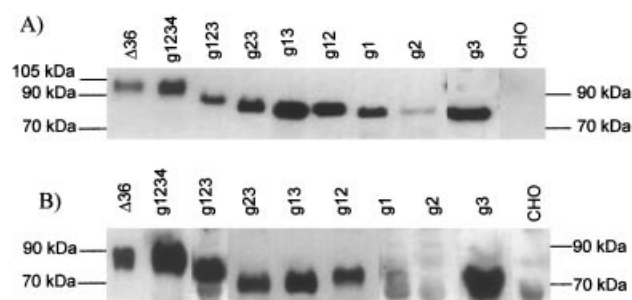


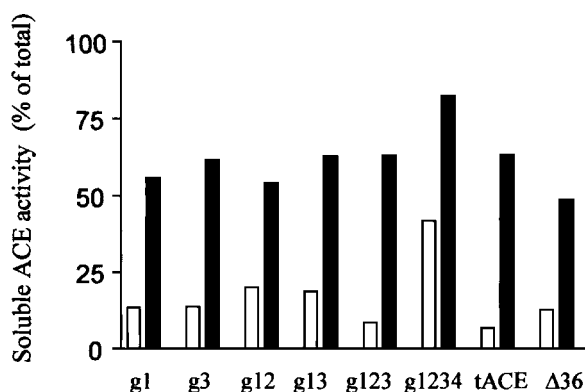
**Figure 2** Expression of tACE $\Delta$ 36 glycosylation mutants

Proteins were immunodetected from detergent-solubilized cells (A) and from harvested medium (B) with rabbit anti-human-tACE antibody (at 1:2000 dilution). The estimated protein sizes are indicated. Lanes contain tACE $\Delta$ 36 ( $\Delta$ 36), ACE glycosylation mutants tACE $\Delta$ 36-g $n$ , where  $n$  represents the N-glycosylation sites (see Figure 1), and untransfected CHO cell control.

**Table 1 Kinetic parameters for the hydrolysis of Hip-His-Leu by various tACE glycoforms**

CHO cells expressing tACE $\Delta$ 36NJ were grown in the presence (+) or absence (–) of the glucosidase-I inhibitor NB-DNJ. Data are means  $\pm$  S.E.M. from triplicates and assay conditions were as described in the Materials and methods section.

tACE glycoform	$K_m$ (mM)	$k_{cat}$ ( $s^{-1}$ )	$k_{cat}/K_m$ ( $s^{-1} \cdot mM^{-1}$ )
tACE	$2.7 \pm 0.67$	$196 \pm 23$	69
tACE $\Delta$ 36-g1	$1.6 \pm 0.40$	$128 \pm 11$	79
tACE $\Delta$ 36-g3	$2.5 \pm 0.67$	$115 \pm 14$	45
tACE $\Delta$ 36-g13	$2.7 \pm 0.82$	$170 \pm 25$	63
tACE $\Delta$ 36-g2	–	–	–
tACE $\Delta$ 36-g12	$2.1 \pm 0.41$	$195 \pm 15$	94
tACE $\Delta$ 36-g123	$2.9 \pm 1.03$	$210 \pm 37$	71
tACE $\Delta$ 36-g1234	$1.5 \pm 0.18$	$85 \pm 3.2$	56
tACE $\Delta$ 36NJ (+NB-DNJ)	$2.6 \pm 0.37$	$253 \pm 15$	99
tACE $\Delta$ 36NJ (–NB-DNJ)	$4.1 \pm 0.47$	$310 \pm 18$	76

**Figure 3 Effect of phorbol ester on the levels of soluble (shed) tACE activity**

Results are expressed as a percentage of total (soluble + cell-associated) ACE activity. Black bars are in the presence and white bars are in the absence of phorbol ester. Results are shown for wild-type tACE (tACE), tACE $\Delta$ 36 ( $\Delta$ 36) and glycosylation mutants tACE $\Delta$ 36-*gn* (see Figure 1).

enzyme. Furthermore, treatment of cells expressing tACE $\Delta$ 36NJ with the glucosidase-I inhibitor NB-DNJ did not alter the kinetic properties of the expressed enzymes (Table 1).

#### Ectodomain shedding of tACE and analysis of juxtamembrane cleavage sites

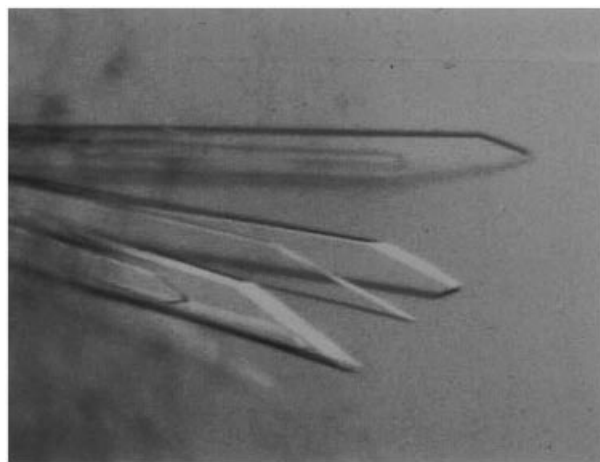
Independent transfections of CHO cells with tACE $\Delta$ 36-g1, -g12, -g123 and -g1234 were performed, which yielded consistent results for each mutant (Figure 3). All glycosylation mutants showed similar levels of phorbol ester stimulation.

Thus N-linked glycosylation did not appear to affect solubilization (i.e. shedding) of the membrane-anchored enzyme. Further protein analysis was performed to (i) identify the C-terminal peptide to determine whether cleavage of tACE $\Delta$ 36-g1, -g13 and -g1234 occurred at the same bond as in tACE and (ii) investigate the glycosylation status of the seventh recognition sequon, which lies seven residues proximal to the tACE cleavage site. The mass spectra of endoproteinase Lys-C-digested peptides of tACE $\Delta$ 36-g1, -g13 and -g1234 revealed three  $[M+H]^+$  ions of

**Table 2 Mass spectral analysis of C-terminal endoproteinase Lys-C peptides**

Soluble (shed) tACE proteins were purified from conditioned medium of transfected CHO cells, digested with endoproteinase Lys-C and analysed by MALDI-TOF MS. Amino acid residue numbering refers to tACE-wt [7]. Shown are the masses of the penultimate (\*) and ultimate (†) C-terminal peptides. All values are calculated for protonated isotopically averaged molecular masses  $m/z$ . In parentheses are the expected masses.

Peptide (residue no.)	tACE $\Delta$ 36-g1	tACE $\Delta$ 36-g13	tACE $\Delta$ 36-g1234	tACE $\Delta$ 36NJ
598–613*	1951.6 (1951.2)	1950.6 (1951.2)	1950.2 (1951.2)	1951.5 (1951.2)
614–627†	1689.7 (1690.8)	1690.5 (1690.8)	1690.9 (1690.5)	
614–625†				1463.1 (1463.5)

**Figure 4 Orthorhombic crystals of tACE $\Delta$ 36NJ**

$m/z$  1689.7, 1690.5 and 1690.9, respectively (Table 2), which were in close agreement with the theoretical mass of the C-terminal peptide (calculated  $m/z$ , 1690.8).

Thus, for tACE $\Delta$ 36-g1, -g13 and -g1234, proteolysis occurred between Arg-627 and Ser-628, which is the same site as in tACE-wt. The spectra of the mutant tACE $\Delta$ 36NJ revealed an  $[M+H]^+$  ion at  $m/z$  1463.1, which corresponded to the calculated mass of the peptide Leu-614–Ser-625, confirming that truncation occurred at Ser-625 and that there was no further limited proteolysis of the C-terminus (Table 2).

#### Crystallization of ACE mutants

We have successfully crystallized tACE $\Delta$ 36NJ (Figure 4), as well as the tACE $\Delta$ 36-g1234 and tACE $\Delta$ 36-g13 mutants, under similar conditions. Crystals usually appeared within 2 weeks and grew to their maximum size after  $\approx$  1 month. The tACE $\Delta$ 36NJ crystals belonged to the orthorhombic P2<sub>1</sub>2<sub>1</sub>2<sub>1</sub> space group, with one molecule in the crystallographic asymmetric unit and some 49% of the crystal volume occupied by the solvent (cell dimensions,  $a = 56.47 \text{ \AA}$ ,  $b = 84.90 \text{ \AA}$ ,  $c = 133.99 \text{ \AA}$ ,  $\alpha = 90^\circ$ ,  $\beta = 90^\circ$  and  $\gamma = 90^\circ$ ). These crystals diffracted to better than 2.0  $\text{\AA}$  resolution on a Synchrotron source. Preliminary diffraction experiments have shown that the tACE $\Delta$ 36-g1234 and tACE $\Delta$ 36-g13 crystals diffracted to at least 2.8 and 3.0  $\text{\AA}$  resolution, respectively, and these crystals were isomorphous with the tACE $\Delta$ 36NJ crystals.

## DISCUSSION

Previous studies established that human tACE $\Delta$ 36NJ expressed in the presence of the glucosidase inhibitor NB-DNJ could be deglycosylated enzymically, while still maintaining its structural and functional integrity. This proved to be a good candidate for crystallization studies, but low yields prompted us to investigate further the expression and crystallization of other tACE $\Delta$ 36 glycoforms.

It is known that the O-linked sugars in human tACE are not necessary for expression, implicating the N-linked sugars in this role [10]. There are seven potential N-linked sites in human tACE, five of which are complementary to the sites in rabbit tACE [5]. The unique sites in human tACE lie within the ectodomain (the fourth site) and in the juxtamembrane stalk region, adjacent to the cleavage site (seventh site). As with the rabbit enzyme, there appears to be a preference for glycosylation at the N-terminus [5]. In the present study, the minimum glycosylation requirements for the expression and processing of enzymically active human tACE were determined by progressive deglycosylation. To investigate which sugars are vital for tACE expression, a series of mutants were constructed that contain a limited number of sites for N-linked glycosylation. N-glycan recognition sequons within the protein sequence were disrupted by mutagenesis of the asparagine to a glutamine residue within the sequon.

Unglycosylated tACE-wt expressed in the presence of tunicamycin is not shed, since it requires the presence of N-glycans for proper expression, maturation and processing (results not shown). However, our studies revealed that the removal of a large percentage of these glycans did not impair the expression of enzymically active tACE $\Delta$ 36, and that the presence of glycans at two of the three N-terminal sites was sufficient to produce protein that retained the kinetic properties of the native enzyme. Furthermore, the minimum N-linked glycosylation that enabled expression of enzymically active tACE was the presence of glycans at either the first or the third site. Glycosylation at either of these sites appeared to be sufficient for protein folding, whereas glycosylation of only the second site resulted in rapid intracellular degradation. This is in agreement with the glycosylation requirements of active rabbit ACE expressed in mammalian cells and in yeast, which also had a minimum requirement of at least one of the three N-terminal sites [11].

Interestingly, in the rabbit enzyme, mutants that had either the first or second site intact were expressed as active proteins. In contrast, glycosylation at the third site alone was not sufficient to produce active protein in HeLa cells, although this mutant was expressed in yeast [11], indicating that glycosylation requirements differ slightly for ACE from different species and are also cell-specific.

In a recent study, Nachon et al. [12] produced a minimally glycosylated recombinant monomeric butyrylcholinesterase (BchE) suitable for X-ray crystallographic studies. They showed that the mutant, lacking four out of nine N-glycosylation sites, as well as the C-terminal tetramerization domain, exhibited similar kinetic parameters to the native enzyme. However, the suppression of sites towards the N-terminus resulted in reduced relative expression levels and intracellular retention of the enzyme. Other glycoproteins that show a similar preference for N-linked glycosylation at the N-terminus include vasoactive intestinal peptide I receptor [13] and parathyroid-related peptide receptor [14].

In the construction of the tACE $\Delta$ 36 glycosylation mutants, the seventh C-terminal site, which is not present in rabbit tACE, was not targeted as it has been shown to be unglycosylated in human

tACE [5]. With the removal of the N-terminal glycosylation sequons it is possible that this site may become glycosylated to compensate for the loss of oligosaccharide chains. However, our MALDI-TOF mass spectra data indicate that this does not occur, since our analyses only revealed the unglycosylated C-terminal peptide containing the seventh glycosylation site.

Generally, there is a preference for oligosaccharides to be attached to sequons containing threonine residues rather than serine residues. This was also observed in human tACE, where all sequons with a serine in the third position were partially glycosylated and those with threonine were fully glycosylated. An exception was the seventh site, which was unglycosylated despite the presence of a threonine in the third position [5]. Oligosaccharyl transferase-mediated attachment of oligosaccharides occurs when the sequon adopts an Asx turn. The tryptophan in the second position of the seventh sequon, which has a bulky aromatic ring in the side chain, may preclude the formation of the Asx turn, thereby preventing glycosylation at this site [15]. This interpretation is supported by the finding that a tACE stalk deletion mutant, tACE- $\Delta$ 6, which generated a novel Asn-Arg-Ser sequon adjacent to the wild-type cleavage site, was glycosylated [16].

Enzymic removal of N-linked glycans was used to produce crystals of CD2 glycoprotein that diffracted to 2.5 Å [17]. However, we found that crystallization trials with deglycosylated tACE $\Delta$ 36NJ that had a single GlcNAc residue attached to the asparagine residue of the N-linked site only produced needle-like crystals that were not suitable for further diffraction studies (E. D. Sturrock, A. C. Papageorgiou and K. R. Acharya, unpublished work).

Surprisingly, tACE $\Delta$ 36NJ expressed in the presence of NB-DNJ, but retaining the simple high-mannose oligosaccharides (Glc<sub>3</sub>Man<sub>7</sub>GlcNAc<sub>2</sub>), yielded the best crystals for X-ray diffraction studies and these have been used to solve the structure of tACE at a resolution of 2.0 Å [18]. The kinetic properties of the tACE $\Delta$ 36NJ mutant were not influenced by NB-DNJ treatment, in accordance with the previous finding that the  $K_m$  values for glycosylated and deglycosylated forms of tACE $\Delta$ 36NJ were identical with the  $K_m$  for tACE-wt, using furanacryloyl-Phe-Gly-Gly as a substrate [5].

Glucosidase inhibitors, at concentrations required to block trimming of the terminal glucose residues and subsequent complex oligosaccharide formation, can affect cell maturation and apoptosis [19]. This treatment also results in a decrease in protein expression (E. D. Sturrock and S. L. Schwager, unpublished work). Therefore, we also used mutants lacking some of the C-terminal N-linked glycans, with the objective of producing proteins with a minimal number of oligosaccharides that would crystallize in a reproducible fashion. Crystals of glycosylation mutants g13 and g1234 were grown under similar conditions to those for tACE $\Delta$ 36NJ. The glycosylation-mutant crystals grew faster than tACE $\Delta$ 36NJ crystals and were smaller in size, but have also proved to be suitable for diffraction work.

In conclusion, our data indicate that the key to producing diffraction-quality crystals of human tACE (which is identical to the C-domain of somatic ACE) consists of reducing the number or the complexity of N-linked oligosaccharides, in addition to deleting the N-terminal 36-residue O-glycosylated sequence and eliminating the C-terminal cytoplasmic and transmembrane domains (recombinantly or by cell-mediated shedding). These modifications produce stable, enzymically active ACE mutants that generate crystals which diffract up to 2.0 Å resolution.

This work was supported by the Wellcome Trust (U.K.) Collaborative Research Initiative grant 054534 to E. D. S. and K. R. A., project grant 060935 to K. R. A. and an NRF (South Africa) grant to E. D. S. We thank the staff at the synchrotron radiation

sources at ESRF, Grenoble, France, and SRS, Daresbury, Cheshire, U.K., for their help with X-ray diffraction data collection. We also thank Dr Fran Platt from the Glycobiology Institute, University of Oxford, Oxford, U.K., for providing the NB-DNJ.

## REFERENCES

- 1 Tipnis, S. R., Hooper, N. M., Hyde, R., Karran, E., Christie, G. and Turner, A. J. (2000) A human homolog of angiotensin-converting enzyme. Cloning and functional expression as a captopril-insensitive carboxypeptidase. *J. Biol. Chem.* **275**, 33238–33243
- 2 Crackower, M. A., Sarao, R., Oudit, G. Y., Yagil, C., Kozieradzki, I., Scanga, S. E., Oliveira-dos-Santos, A. J., da Costa, J., Zhang, L., Pei, Y. et al. (2002) Angiotensin-converting enzyme 2 is an essential regulator of heart function. *Nature (London)* **417**, 822–828
- 3 Waller, C. L. and Marshall, G. R. (1993) Three-dimensional quantitative structure-activity relationship of angiotensin-converting enzyme and thermolysin inhibitors. II. A comparison of CoMFA models incorporating molecular orbital fields and desolvation free energies based on active-analog and complementary-receptor-field alignment rules. *J. Med. Chem.* **36**, 2390–2403
- 4 Mayer, M. and Meyer, B. (2000) Mapping the active site of angiotensin-converting enzyme by transferred NOE spectroscopy. *J. Med. Chem.* **43**, 2093–2099
- 5 Yu, X. C., Sturrock, E. D., Wu, Z., Biemann, K., Ehlers, M. R. and Riordan, J. F. (1997) Identification of N-linked glycosylation sites in human testis angiotensin-converting enzyme and expression of an active deglycosylated form. *J. Biol. Chem.* **272**, 3511–3519
- 6 Ehlers, M. R., Schwager, S. L., Scholle, R. R., Manji, G. A., Brandt, W. F. and Riordan, J. F. (1996) Proteolytic release of membrane-bound angiotensin-converting enzyme: role of the juxtamembrane stalk sequence. *Biochemistry* **35**, 9549–9559
- 7 Ehlers, M. R., Fox, E. A., Strydom, D. J. and Riordan, J. F. (1989) Molecular cloning of human testicular angiotensin-converting enzyme: the testis isozyme is identical to the C-terminal half of endothelial angiotensin-converting enzyme. *Proc. Natl. Acad. Sci. U.S.A.* **86**, 7741–7745
- 8 Schwager, S. L., Chubb, A. J., Scholle, R. R., Brandt, W. F., Eckerskorn, C., Sturrock, E. D. and Ehlers, M. R. (1998) Phorbol ester-induced juxtamembrane cleavage of angiotensin-converting enzyme is not inhibited by a stalk containing intrachain disulfides. *Biochemistry* **37**, 15449–15456
- 9 Wei, L., Alhenc-Gelas, F., Corvol, P. and Clauser, E. (1991) The two homologous domains of human angiotensin I-converting enzyme are both catalytically active. *J. Biol. Chem.* **266**, 9002–9008
- 10 Ehlers, M. R., Chen, Y. N. and Riordan, J. F. (1992) The unique N-terminal sequence of testis angiotensin-converting enzyme is heavily O-glycosylated and unessential for activity or stability. *Biochem. Biophys. Res. Commun.* **183**, 199–205
- 11 Sadhukhan, R. and Sen, I. (1996) Different glycosylation requirements for the synthesis of enzymatically active angiotensin-converting enzyme in mammalian cells and yeast. *J. Biol. Chem.* **271**, 6429–6434
- 12 Nachon, F., Nicolet, Y., Viguie, N., Masson, P., Fontecilla-Camps, J. C. and Lockridge, O. (2002) Engineering of a monomeric and low-glycosylated form of human butyrylcholinesterase: expression, purification, characterization and crystallization. *Eur. J. Biochem.* **269**, 630–637
- 13 Couvineau, A., Fabre, C., Gaudin, P., Maoret, J. J. and Laburthe, M. (1996) Mutagenesis of N-glycosylation sites in the human vasoactive intestinal peptide 1 receptor. Evidence that asparagine 58 or 69 is crucial for correct delivery of the receptor to plasma membrane. *Biochemistry* **35**, 1745–1752
- 14 Zhou, A. T., Assil, I. and Abou-Samra, A. B. (2000) Role of asparagine-linked oligosaccharides in the function of the rat PTH/PTHrP receptor. *Biochemistry* **39**, 6514–6520
- 15 Imperiali, B. and O'Connor, S. E. (1999) Effect of N-linked glycosylation on glycopeptide and glycoprotein structure. *Curr. Opin. Chem. Biol.* **3**, 643–649
- 16 Schwager, S. L., Chubb, A. J., Scholle, R. R., Brandt, W. F., Mentele, R., Riordan, J. F., Sturrock, E. D. and Ehlers, M. R. (1999) Modulation of juxtamembrane cleavage ("shedding") of angiotensin-converting enzyme by stalk glycosylation: evidence for an alternative shedding protease. *Biochemistry* **38**, 10388–10397
- 17 Davis, S. J., Davies, E. A., Barclay, A. N., Daenke, S., Bodian, D. L., Jones, E. Y., Stuart, D. I., Butters, T. D., Dwek, R. A. and van der Merwe, P. A. (1995) Ligand binding by the immunoglobulin superfamily recognition molecule CD2 is glycosylation-independent. *J. Biol. Chem.* **270**, 369–375
- 18 Natesh, R., Schwager, S. L. U., Sturrock, E. D. and Acharya, K. R. (2003) Crystal structure of the human angiotensin-converting enzyme-lisinopril complex. *Nature (London)* **421**, 551–554
- 19 Misago, M., Tsukada, J., Fukuda, M. N. and Eto, S. (2000) Suppressive effects of swainsonine and N-butyldeoxynojirimycin on human bone marrow neutrophil maturation. *Biochem. Biophys. Res. Commun.* **269**, 219–225

Received 26 November 2002/22 January 2003; accepted 24 January 2003

Published as BJ Immediate Publication 24 January 2003, DOI 10.1042/BJ20021842